8656 *Biochemistry* **2009,** *48,* 8656–8663
DOI: 10.1021/bi900239b

BIOCHEMISTRY
including biophysical chemistry & molecular biology
Article

Impaired Protofibril Formation in Fibrinogen γN308K Is Due to Altered D:D and "A:a" Interactions[†,‡]

Sheryl R. Bowley,[§] Nobuo Okumura,[∥] and Susan T. Lord*[,§,⊥]

[§]*Department of Chemistry and* [⊥]*Department of Pathology and Laboratory Medicine, University of North Carolina at Chapel Hill, Chapel Hill, North Carolina 27599, and* [∥]*Department of Biomedical Laboratory Sciences, Shinshu University, Matsumoto, Japan*

Received February 13, 2009; Revised Manuscript Received July 30, 2009

ABSTRACT: "A:a" knob−hole interactions and D:D interfacial interactions are important for fibrin polymerization. Previous studies with recombinant γN308K fibrinogen, a substitution at the D:D interface, showed impaired polymerization. We examined the molecular basis for this loss of function by solving the crystal structure of γN308K fragment D. In contrast to previous fragment D crystals, the γN308K crystals belonged to a tetragonal space group with an unusually long unit cell ($a = b = 95$ Å, $c = 448.3$ Å). Alignment of the normal and γN308K structures showed the global structure of the variant was not changed and the knob "A" peptide GPRP was bound as usual to hole "a". The substitution introduced an elongated positively charged patch in the D:D region. The structure showed novel, symmetric D:D crystal contacts between γN308K molecules, indicating the normal asymmetric D:D interface in fibrin would be unstable in this variant. We examined GPRP binding to γN308K in solution by plasmin protection assay. The results showed weaker peptide binding, suggesting that "A:a" interactions were altered. We examined fibrin network structures by scanning electron microscopy and found the variant fibers were thicker and more heterogeneous than normal fibers. Considered together, our structural and biochemical studies indicate both "A:a" and D:D interactions are weaker. We conclude that stable protofibrils cannot assemble from γN308K monomers, leading to impaired polymerization.

Fibrinogen is a 340 kDa plasma glycoprotein composed of six polypeptide chains, (Aα, Bβ, γ)$_2$, folded into three distinct structural regions: two distal D regions linked by coiled-coil connectors to one central E region forming a trinodular molecule (see Figure 1) (*1*). The symmetric D regions contain the polymerization holes "a" and "b" located in the C-terminus of the γ- and Bβ-chains, respectively. The central E region contains two sets of polymerization knobs "A" and "B" that are cryptic in fibrinogen but become exposed in fibrin after thrombin cleaves fibrinopeptides A (FpA) and B (FpB) from the N-terminus of the Aα- and Bβ-chains, respectively. In the proposed model of polymerization (Figure 1) (*1*), the exposed knobs "A", which start with the sequence Gly-Pro-Arg-, bind to holes "a" in two other fibrin molecules forming "A:a" interactions. Because the fibrin monomers are symmetric, these and the reciprocal "A:a" interactions lead to a double-stranded protofibril with a half-staggered overlap between molecules in different strands. The end-to-end alignment of monomers in each protofibril strand abuts the γ-chains of two adjacent molecules to form the D:D interface. Subsequently, FpB is released, and the protofibrils assemble in three dimensions to form a branched network of fibers. The fibrin network is stabilized by the transglutaminase FXIIIa, which catalyzes formation of intermolecular cross-links between fibrin monomers. Because cross-links form between γ-chains, it is possible to isolate a fibrin fragment, called double-D, containing the D:D interface.

Even though the adjoined D regions are identical, crystallography studies have shown the D:D interface in double-D is asymmetric (Figure 1). The asymmetric interactions include only a few potential hydrogen bonds and no obvious salt links (*2*). The functional significance of these interactions is evident in several dysfibrinogenemia cases involving substitution at one residue within the D:D interface, γ308Asn. Patients with a Lys substitution, γN308K, have been associated with thrombosis or bleeding (*3*). Fibrinogen Kyoto I was isolated from a hypofibrinogenemic patient who had a family history of both thrombosis and bleeding (*4*). Fibrinogen Bicetre II was found in a patient who suffered pulmonary embolism (*5*). Fibrinogen Matsumoto II was isolated from a patient with a history of severe bleeding (*6*). In contrast, the Ile substitution, γN308I, was identified in an asymptomatic patient (fibrinogen Baltimore III) (*7*).

Biochemical analysis of recombinant fibrinogens γN308K, γN308I, and γN308A showed all three had impaired polymerization in the absence of added calcium (*8*). At 0.1 mM calcium, polymerization of both γN308I and γN308A was nearly normal while polymerization of γN308K remained markedly impaired even at 5 mM calcium. FXIIIa-catalyzed γ−γ dimer formation was also significantly delayed in γN308K. These studies suggest that a critical aspect of polymerization in conjunction with calcium binding is disrupted in γN308K (*8*). Nevertheless, calcium binding studies with γN308K fragment D derived from the Kyoto patient's fibrinogen showed essentially identical binding when compared to normal fragment D (*9*). Although γ308Asn is located at the D:D interface, crystal structures show

[†]This work was supported by National Institutes of Health Grant HL 31048 (to S.T.L.). S.R.B. is supported by an American Heart Association Predoctoral Fellowship, 0715292U.

[‡]The atomic coordinates have been deposited in the Protein Data Bank (www.rcsb.org) under the access code 3HUS (rfD-γN308K + GP).

*Corresponding author. Phone: (919) 966-3548. Fax: (919) 966-6718. E-mail: stl@med.unc.edu.

 Published on Web 08/03/2009

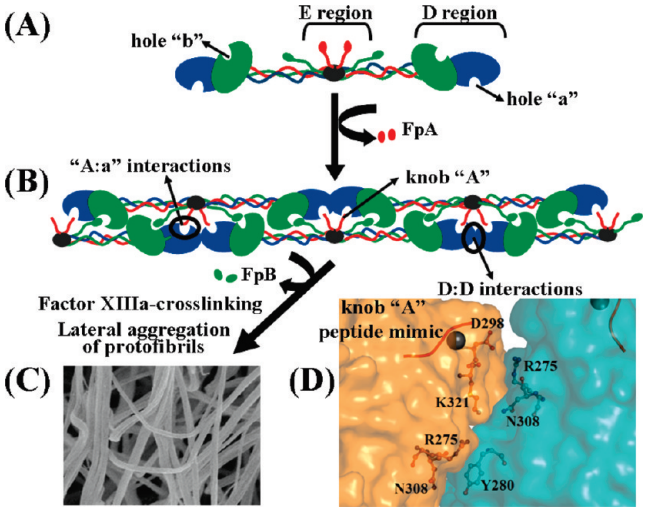

FIGURE 1: Schematic representation of fibrin polymerization. Fibrinogen (A) is a dimer of three polypeptide chains, Aα (in red), Bβ (in green), and γ (in blue). Removal of fibrinopeptides A (FpA) in the central E region of the molecule exposes knobs "A" which bind to holes "a" in the γ-chain, leading to the formation of protofibrils (B). Fibrin networks (C) form after lateral aggregation of protofibrils. Factor XIIIa catalyzes the cross-linking of fibrin molecules. Because cross-links form between neighboring γ-chains, it is possible to isolate a fragment, called double-D, that contains the D:D interface. Crystallography studies of the double-D show the D:D interface is asymmetric (D).

this residue is also near polymerization hole "a" and the calcium binding site, γ1. Whether or not the γN308K substitution impacts the D:D interface, "A:a" interactions, or γ1 calcium binding remains unclear.

In this study, we examined the structural basis for the functional impairment of γN308K. We crystallized fragment D from γN308K in the presence of the peptide GPRP, which mimics knob "A", and solved the 3.05 Å structure (rfD-γN308K + GP, PDB code 3HUS). We characterized calcium binding and "A:a" interactions in γN308K using a plasmin protection assay. We performed scanning electron microscopy to examine the variant clot structure. Our biochemical and structural data suggest γ308Asn is critical for stable protofibril formation, not only for the D:D interface that forms during end-to-end association of fibrin molecules but also for the structural integrity of loops that influence "A:a" knob−hole interactions.

EXPERIMENTAL PROCEDURES

Reagents. All chemicals were of reagent grade and were purchased from Sigma-Aldrich (St. Louis, MO), unless specified otherwise. The peptide GPRP-amide was purchased from Bachem Americas, Inc. (Torrance, CA). Cell culture media with normal recombinant fibrinogen were obtained from the National Cell Culture Center (Minneapolis, MN). Monoclonal IF-1 antibody was purchased from Kamiya Biomedical (Seattle, WA). All molecular graphics were illustrated using PyMol (DeLano Scientific LLC, Palo Alto, CA).

Expression and Purification of Recombinant γN308K. Normal and variant fibrinogen γN308K were synthesized in CHO cells as described (*8*). Large-scale protein expression was carried out in serum-free medium in roller bottles. Media containing secreted fibrinogen were harvested periodically. After addition of protease inhibitors, the media were stored at −20 °C .

Recombinant fibrinogen was purified as described (*10*). Briefly, fibrinogen was precipitated from the media with ammonium sulfate in the presence of protease inhibitors. The precipitate was resuspended in buffer containing 10 mM $CaCl_2$ and applied to a Sepharose 4B column coupled with the calcium-dependent monoclonal antibody, IF-1. Fibrinogen was eluted with 5 mM EDTA, dialyzed once against 20 mM HEPES, pH 7.4, 150 mM NaCl (HBS), and 1 mM $CaCl_2$. The protein was extensively dialyzed against HBS and then stored at −80 °C. The integrity of the polypeptides and the purity of the recombinant protein were analyzed by SDS−PAGE under reduced and nonreduced conditions following the method of Laemmli (*11*).

Preparation and Purification of Fragment D. Fragment D was prepared from γN308K by controlled trypsin digestion as described (*12*, *13*). Briefly, $CaCl_2$ (final concentration of 20 mM) was added to 10 mg of γN308K at 0.7 mg/mL in HBS, and digestion was initiated by adding a 100 μL slurry of bead-immobilized TPCK trypsin (Pierce Biotechnology Inc., Rockford, IL). The reaction proceeded over a period of days at room temperature until SDS−PAGE revealed essentially two bands that correspond to the molecular weights of fragments D and E. Digestion was stopped by removing the trypsin beads with centrifugation at 1200 × *g* (Sorvall RC-3) for 10 min. Fragment D was purified by peptide affinity chromatography as described with modification (*12*, *13*). Briefly, the digest was loaded onto a polymeric resin covalently linked to the peptide GPRPAA. Fragment D was eluted using 50 mM sodium acetate, pH 5.3, and 1 M NaBr. Purified fragment D was dialyzed against 50 mM Tris-HCl, pH 7.4, then concentrated to about 30 mg/mL with a centrifugal filter device (50 kDa MW cutoff; Millipore Corp., Billerica, MA), and stored at 4 °C.

Crystallization of γN308K Fragment D. Purified γN308K fragment D was cocrystallized with GPRP by sitting-drop diffusion at 4 °C as previously described (*2*, *12*, *13*). Crystals were grown from drops containing 5 μL of γN308K fragment D at 10 mg/mL in 50 mM Tris-HCl, pH 7.4, and GPRP at 5 mM. The protein−peptide solution was mixed with 5 μL of crystallization solution containing 50 mM Tris-HCl, pH 8.5, 2 mM NaN_3, 12.5 mM $CaCl_2$, and 9% (w/v) PEG 3350. Single crystals appeared in days, following streak seeding with crystals of normal recombinant fragment D.

X-ray Diffraction Data Collection and Structure Determination. Data collection for crystals of γN308K fragment D cocrystallized with GPRP (rfD-γN308K + GP) was carried out at 100 K using beamline X29A at the National Synchrotron Light Source at Brookhaven National Laboratory. A single crystal was cryoprotected in a loop containing the crystallant solution plus 20% glycerol and 5 mM GPRP and then flash-frozen in liquid nitrogen. Initial screening revealed the crystal had a long *c* cell edge; hence, oscillation data were recorded at a crystal-to-detector distance of 350 mm to achieve adequate diffraction spot separation. The data were processed with DENZO and scaled in ScalePack (*14*).

The native Patterson map showed a large peak at fractional coordinates of (0, 0, 0.472) suggesting the presence of a translational noncrystallographic symmetry (NCS). To generate a model for molecular replacement, the coordinates of one molecule of the normal recombinant fragment D (PDB code 1LT9) were used as a starting point. Using the Superpose program in CCP4 (*15*), another copy of the molecule was generated by translation using the orthogonal coordinates (0, 0, 0.472*c*), where *c* is the length of the *c* cell edge (448.3 Å). The coordinates of the

original and the translated molecules were put together to make up a new model consisting of two molecules separated by the NCS translation. Using the automated search mode in PHASER (*16*) and the two-molecule search model, the structure of rfD-γN308K + GP was solved. The resulting model was refined using Refmac 5 (*17*), reserving 5% of the reflections for the calculation of the R_{free} factor. After one round of refinement, the model was improved by manual fitting with the program Coot (*18*) using sigmaA-weighted $|2F_o - F_c|$ and $|F_o - F_c|$ electron density maps (*19*). Water molecules and *cis*-peptide bonds were added at positions Bβ407 and γ339 to complete the model. Final refinement was done with the TLS protocol in Refmac 5 (*20*). After these refinement steps, the R_{cryst} and R_{free} converged to the values reported in Table 1.

Analysis of the Molecular Packing in γN308K. Because γ308Asn involves mutation at the D:D interface of adjacent fibrin units, we examined the molecular packing of rfD-γN308K + GP using MSDPisa (*21*). We analyzed the D:D crystal contacts of the recombinant fragment D structures and compared these to the actual D:D interface observed in the FXIIIa cross-linked double-D structure.

Scanning Electron Microscopy (*SEM*). Specimen preparations were based on a previously described method with some modifications (*22*). For each polymerization condition, SEM was performed on two clots each with two separate microscopy preparations for normal and γN308K fibrinogen. Clots (100 μL) were polymerized for 4 h in 96-well microtiter plates using 0.5 mg/mL fibrinogen and 0.4 unit/mL thrombin in HBS without added $CaCl_2$ or with 5 mM $CaCl_2$. The clots were fixed in 2% glutaraldehyde overnight, rinsed three times with HBS, and dehydrated with a series of ethanol solutions (20−100%). The samples were dried in a Samdri-795 critical point dryer (Rockville, MD), mounted, sputter-coated with approximately 20 nm of gold−palladium, and viewed on a Zeiss Supra 25 FESEM (Carl Zeiss MicroImaging, Inc., Thornwood, NY). Images were taken at high (101000×) and low (21000×) magnifications, with a 9.0 mm working distance and 5 kV accelerating voltage. Fiber diameters were measured from the high magnification images using the measurement tool in Photoshop (Adobe Systems, San Jose, CA).

Plasmin Protection Assay. This assay was adapted from previous studies (*23*). To examine calcium binding, $CaCl_2$ or EDTA (at 5 mM final concentration) was added to 5 μg of fibrinogen at 0.2 mg/mL in HBS. To examine GPRP binding, varying concentrations of the peptide (2 μM, 20 μM, 0.1 mM, 0.5 mM, 1 mM, 5 mM, and 20 mM) were added to 5 μg of fibrinogen at 0.36 mg/mL in HBS supplemented with 5 mM EDTA. Reactions were initiated by adding 2 μL of plasmin (Haematologic Technologies, Inc., Essex Junction, VT) to a final concentration of 4.8 μg/mL. The reaction was incubated for 4 h at 37 °C and then stopped by adding SDS−PAGE loading buffer and heating at 100 °C for 5 min. The plasmin digests were analyzed by nonreducing SDS−PAGE (7.5% gels).

RESULTS

Structure of rfD-γN308K + GP. We obtained the crystal structure of γN308K fragment D with bound GPRP at 3.05 Å (see Table 1). While many crystal structures of fragment D had an orthorhombic space group ($P2_12_12_1$) (*12*, *13*, *24*−*28*), rfD-γN308K + GP had a tetragonal unit cell ($P4_32_12$) with dimensions $a = b = 95$ Å and $c = 448$ Å. The native Patterson map indicated a translational noncrystallographic symmetry, which prompted us to adopt a different strategy for molecular replacement as described in Experimental Procedures. The resulting structure solution gave a rotation and translation *Z* scores of 47.5 and 53.8, respectively. The R_{cryst} and R_{free} values prior to any refinement were 42.6 and 41.5, respectively.

Table 1: Crystallographic Data and Refinement Statistics[a]

data statistics	
resolution (Å)	50.0−3.05 (3.12−3.05)
space group	$P4_32_12$
cell constants *a*, *b*, *c* (Å)	95.0, 95.0, 448.3
molecules/asymmetric unit	2
total observations	324588
unique reflections	40798
mean redundancy	8.0
R_{sym}[b] (%)	14.0 (54.3)
completeness (%)	99.8 (99.9)
mean I/σ	22.8 (4.0)
refinement statistics	
R_{cryst}[c] (%)	23.5
R_{free}[d] (%)	29.5
average *B* factor (Å^2)	61.8
no. of model atoms	10711
no. of solvent sites	101
rms deviations from ideals	
bond length (Å)	0.007
bond angles (deg)	1.04
Ramachandran statistics	
most favored region (%)	91.6
additionally allowed region (%)	8.2

[a]Values in parentheses are statistics for the highest resolution shell. [b]$R_{sym} = \sum|I - \langle I\rangle|$, where *I* is the observed intensity and $\langle I\rangle$ is the average intensity of multiple symmetry-related observations of that reflection. [c]$R_{cryst} = \sum(|F_o| - |F_c|)/\sum|F_o|$, where F_o and F_c are the observed and calculated structure factors, respectively. [d]R_{free} is the *R*-factor based on the 5% of the data withheld from structural refinement.

The change from asparagine to lysine at position γ308 was evident from the negative $|F_o - F_c|$ density around the carboxamide group when asparagine was modeled. Alignment of normal rfD (PDB code 1LT9) and rfD-γN308K + GP showed excellent agreement with rmsd = 0.73 Å over Cα atomic positions. Thus, the global structure of γN308K fragment D was not changed by the substitution. The substitution altered the charge distribution over the surface that makes up the D:D interface, introducing an elongated positively charged patch in γN308K compared to normal.

The rfD-γN308K + GP structure showed GPRP was bound to hole "a" (Figure 2A). This was evident by the presence of positive electron density in $|F_o - F_c|$ maps corresponding to the peptide bound in the hole when GPRP was not modeled. Comparison of the rfD-γN308K + GP structure with several fragment D structures showed only a subtle difference in the conformation of GPRP in hole "a", well within the reported variations in "knob−hole" structures. GPRP was also bound to hole "b" (Figure 2B). These "A:b" interactions have been seen in previous structures of D fragments cocrystallized with just the knob "A" peptide (*25*, *29*). The data in Figure 2 also show calcium was present in the high-affinity calcium binding site in the γ-chain (γ1) of rfD-γN308K + GP. The ion was ~22 Å away from γ308Lys. Calcium was also present at the homologous position in the β-chain, designated as β1 site.

Crystal Packing in rfD-γN308K + GP. We compared the molecular packing in rfD-γN308K + GP crystals to those for normal fragment D and several variant fragment D crystals.

In contrast to all previous crystals, the D:D crystal contacts between γN308K molecules were symmetric (Figure 3). For example, γ241Ala on one molecule is adjacent to γ279Ala on the second, while γ241Ala on the second lies adjacent to γ279Ala in the first. This finding is unique even among crystals of variant fibrinogens. Crystals of fragment D from a variant with an altered hole "a" (PDB code 3BVH), or an altered hole "b" (PDB code 3E1I), and variants with altered calcium binding sites (PDB codes 1RE3, 1RE4, 1RF0, and 1RF1; data not shown) all showed asymmetric D:D crystal contacts similar to those in the normal fragment D crystals with (PDB code 1LTJ) or without (PDB code 1LT9) peptide ligands (Figure 3). This finding suggests that the structure of the γN308K molecule is not conducive to the formation of the normal, asymmetric D:D interface. As previously noted by Everse et al. (*30*), the D:D contacts between individual fragment D molecules in crystals are remarkably similar to the actual D:D interface of the FXIIIa cross-linked double-D fragment. Because the structure of cross-linked double-D is thought to represent the D:D interfacial interactions in protofibrils, they concluded that the crystallographic D:D contacts represent those in fibrin protofibrils. Following this reasoning, our observation that the crystal contacts in rfD-γN308K + GP, being different from all others, suggests this variant cannot form the D:D interface of normal protofibrils. The symmetric D:D crystal contacts between γN308K fragment D molecules involves new set of residues (Figure 3). While the normal asymmetric interface involves residues within γ266−308, many of the contacts in rfD-γN308K + GP occur at the C-terminal end of the γ-chain (γ389−394).

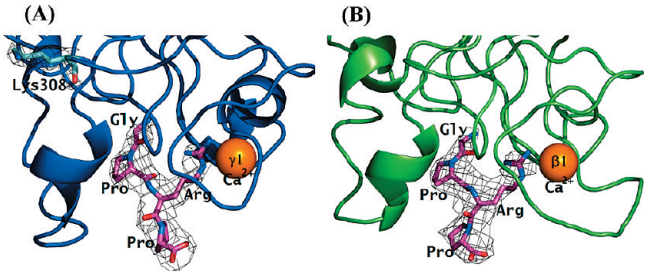

FIGURE 2: Peptide binding in rfD-γN308K + GP. Knob "A" peptide mimic, GPRP (magenta sticks), was bound to hole "a" in the γ-chain (A) and to hole "b" in the β-chain (B), as shown from the $|F_o - F_c|$ maps calculated by omitting the coordinates of the peptide. Also shown are two calcium ions (orange spheres) in the γ1 and β1 calcium binding sites.

Plasmin Protection Assay. Because γ308Asn is close to the γ1 calcium site and hole "a", we examined binding of calcium or GPRP to γN308K using a plasmin protection assay. As previously shown, plasmin proteolysis of normal fibrinogen was limited in the presence of calcium or GPRP (Figure 4A) (*31*, *32*). In the presence of calcium, the main cleavage product was

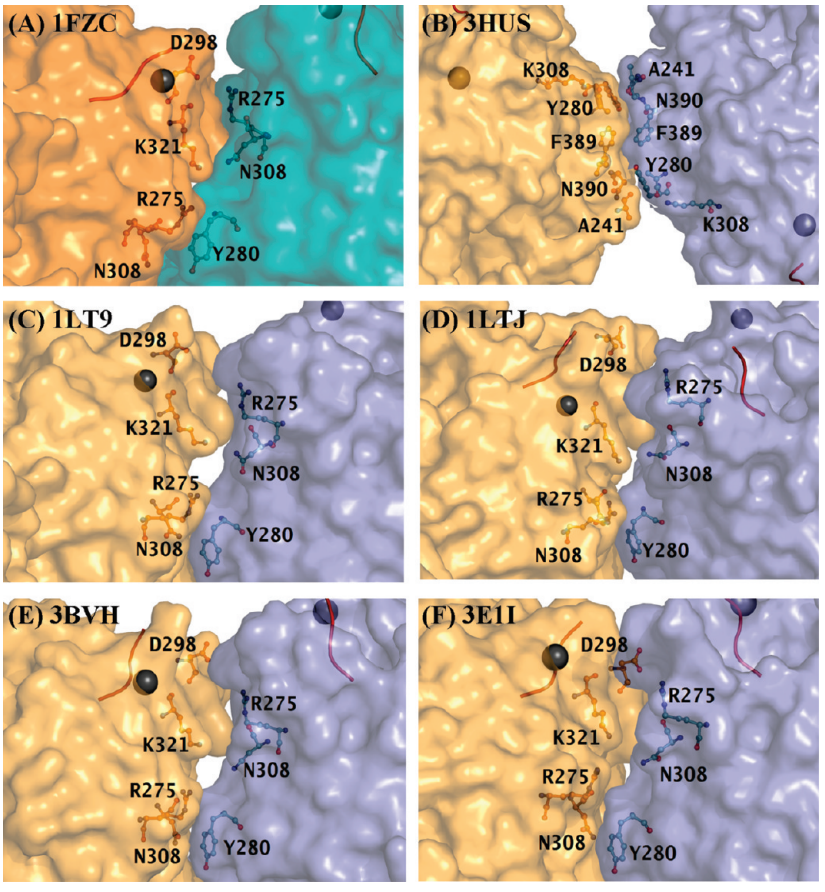

FIGURE 3: Comparison of end-to-end contacts observed in fragment D structures. In all prior fragment D structures (C−F) the crystal contacts were asymmetric and resembled the D:D interface in the naturally cross-linked double-D structure (A). In contrast, rfD-γN308K + GP, PDB code 3HUS (B), showed symmetric end-to-end contacts involving a different set of residues. Calcium ions in the γ1 binding site are shown as gray spheres while the peptide ligands bound to hole "a" are shown in red. Structures shown above are as follows: (A) 1FCZ, cross-linked double-D crystallized with GPRP and knob "B" peptide mimic, GHRP; (B) 3HUS, variant fragment D from γN308K with GPRP; (C) 1LT9, normal recombinant fragment D crystallized without peptides; (D) 1LTJ, normal recombinant fragment D crystallized with GPRP and GHRP; (E) 3BVH, variant fragment D from γD364A with GPRP; (F) 3E1I, variant fragment D from Bβ D432A with GHRP.

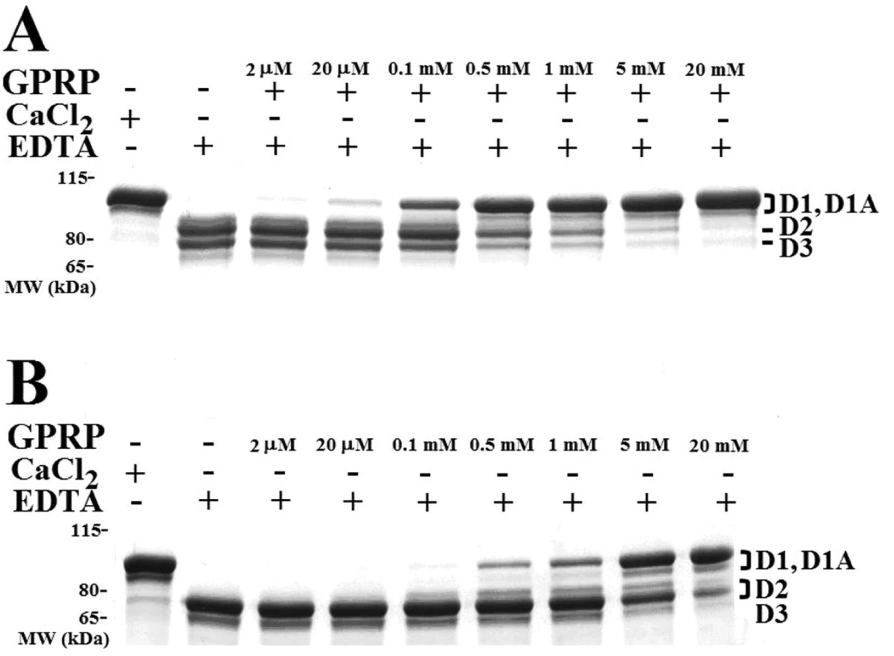

FIGURE 4: Plasmin protection assay analyzed by SDS−PAGE. Normal recombinant (A) or γN308K (B) fibrinogen (~5 μg) containing 5 mM $CaCl_2$, 5 mM EDTA, or increasing GPRP concentration (supplemented with 5 mM EDTA) was incubated with 6 μg/mL plasmin for 4 h at 37 °C. The digests were analyzed under nonreducing conditions on 7.5% gels. Plasmin cleavage products are indicated on the right. The smaller fragments in γN308K may include cleavage at residue 308; thus these are labeled D_2 and D_3 (*9*). Of note, digests of recombinant fibrinogen produce two fragments in the presence of calcium (*13*); we labeled these D_1 and D_{1A}.

fragment D_1. In the presence of EDTA, fragment D_1 was further cleaved into the smaller fragments D_2 and D_3. Similar to normal fibrinogen, fragment D_1 was the predominant product for γN308K in the presence of 5 mM $CaCl_2$, and the addition of 5 mM EDTA led to further digestion into D_2 and D_3 (Figure 4B). These data are consistent with earlier experiments (*9*) that showed calcium binding to fragment D from γN308K dysfibrinogen Kyoto I (K_d = 3.2 μM) was the same as to fragment D from normal fibrinogen (K_d = 2.8 μM). Of note, the γN308K cleavage products that we labeled D_2 and D_3 likely include cleavage at γ308K, as previously reported (*9*).

To assess binding of GPRP, we monitored proteolysis as a function of peptide concentration. With normal fibrinogen, fragment D_1 was readily evident at 20 μM GPRP, suggesting partial protection at this peptide concentration (Figure 4A). The ratio of D_1 to D_2 and D_3 increased with increasing peptide concentration, and full protection was achieved for normal fibrinogen at 5 mM GPRP. In contrast, for γN308K, fragment D_1 was readily evident at 0.5 mM GPRP (Figure 4B). Although the ratio of D_1 to D_2 and D_3 increased with higher peptide concentrations, full protection was not seen even at 20 mM GPRP. These findings suggest that "A:a" interactions in γN308K are about 10-fold weaker than normal.

Scanning Electron Microscopy of Clots. Previous studies examined the polymerization of γN308K as changes in turbidity and found that adding calcium did not markedly alter polymerization of this variant (*8*). To determine whether the final turbidity accurately reflects the variant clot structure, we performed scanning electron microscopy on clots at two calcium concentrations. As shown in Figure 5A, in the absence of calcium, γN308K clots had thicker fibers (160 ± 45 nm) compared to normal (79 ± 18 nm, $p < 0.05$). Moreover, when we compared fiber size distribution by grouping fiber diameters into 10 nm bins, we found a broader, apparently bimodal, distribution of fiber diameters for the γN308K variant. As shown in Figure 5B, with 5 mM calcium the average fiber diameter for normal clots increased to 99 ± 21 nm ($p < 0.05$), as anticipated.

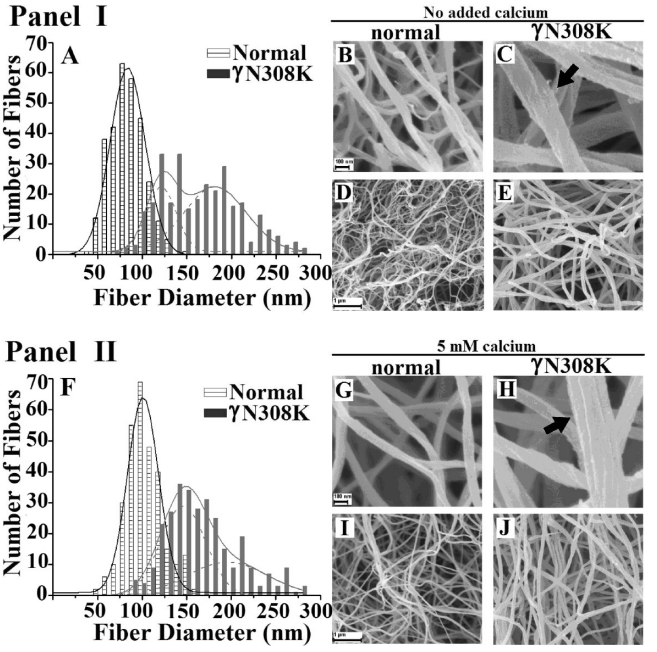

FIGURE 5: Scanning electron micrographs and fiber size distribution of γN308K clots. Fibrinogen (0.5 mg/mL) was incubated with 0.4 unit/mL thrombin without added calcium (panel I) and with 5 mM $CaCl_2$ (panel II) for 4 h at 37 °C. Images of normal (B, D, G, I) and γN308K (C, E, H, J) were recorded at 101000× (B, C, G, and H) and 21000× (D, E, I, and J) magnifications. The black bar scale represents 100 nm for high magnification and 1 μm for lower magnification images. Black arrows indicate thinner fibers in γN308K that twist together like cables to form thicker fiber bundles. Fiber size distribution was determined by grouping fiber diameters into 10 nm wide bins starting with 20 nm and ending with 300 nm. The Gaussian fit curves in (A) and (F) were generated using Origin (Northampton, MA).

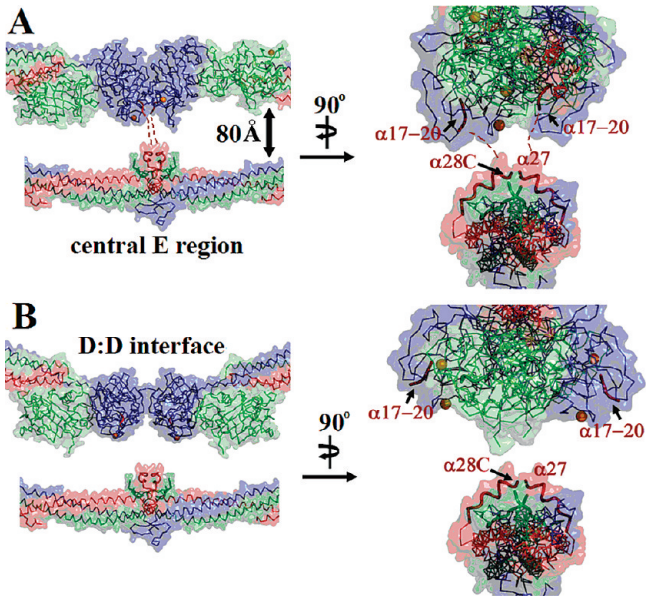

FIGURE 6: Models of protofibril interactions in normal and γN308K. These illustrations build on the model of a protofibril proposed by Yang et al. (*38*). The D:D association in the normal double-D structure (A) allows close proximity between two adjacent holes "a" such that the distance between the bound knob A (α17−20) to the central E region is within the extended length of six residues (dashed red line; missing in the structure) and within the constraints imposed by the α28Cys−α28Cys disulfide bond. In γN308K (B), the different D:D interface puts the two holes "a" in opposite sides of the junction approximately 50 Å away from the central E region, a distance that α17−26 cannot span given the constraints of the α28Cys disulfide bond.

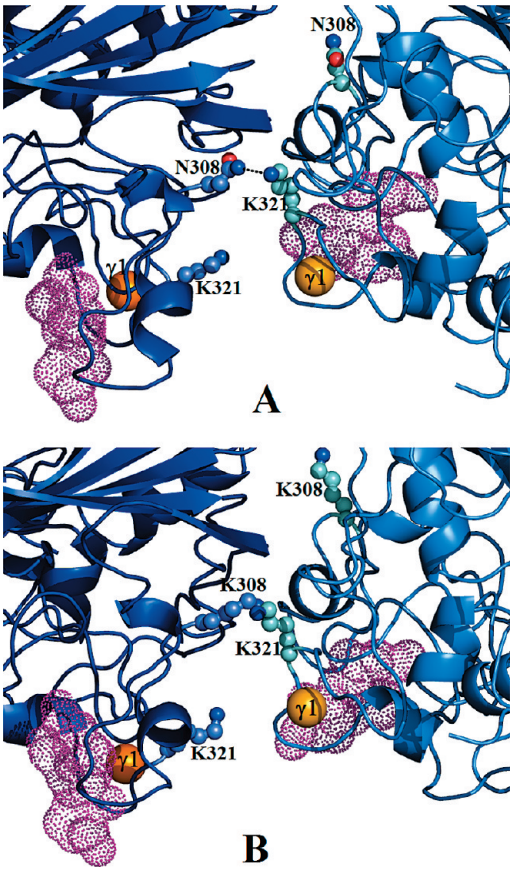

FIGURE 7: Modeling rfD-γN308K + GP into the normal double-D structure. Because the structure of γN308K double-D is not available, individual γN308K fragment D was modeled into the normal double-D structure (A). The γN308K double-D model (B) showed very close proximity between γ308Lys and γ321Lys with a distance of ~2 Å.

In contrast, calcium did not significantly alter the fiber diameter for γN308K (158 ± 40 nm, $p = 0.8$). Fibers in the variant clots were still significantly larger than normal, and the distribution of diameters remained broader than the distribution for normal clots. Of note, in many images the thinner fibers in γN308K clots twist together like cables to form thicker fiber bundles.

DISCUSSION

Taken together, our biochemical and structural studies suggest that stable protofibrils cannot assemble from γN308K monomers, leading to impaired polymerization. Plasmin protection assays showed "A:a" interactions are weaker than normal. The increased surface positive charge and the unique molecular packing in the γN308K fragment D crystals suggest that normal D:D interactions are destabilized by this substitution. As "A:a" and D:D interactions are thought to support protofibril formation, we conclude that monomer assembly into protofibrils is impaired in this variant. This conclusion is consistent with the findings of Okumura et al. (*8*). FXIIIa-catalyzed cross-linking, which normally occurs coincident with protofibril formation, is delayed for γN308K. FpB release, which occurs subsequent to protofibril formation, is also delayed. The influence of calcium on polymerization is diminished, consistent with previous findings that suggest the release of FpB is tied to the calcium dependence of polymerization (*22*). It is notable, however, that polymerization of γN308K fibrinogen is modestly impaired relative to other singly substituted γ-chain variants that directly target either hole "a" (*33*) or the γ1 calcium binding site (*23*).

It is remarkable that the D:D crystal contacts in γN308K are symmetric. In all previously reported normal and variant fragment D structures, the D:D crystal contacts between individual molecules are similar to one another (Figure 3). Moreover, these contacts are similar to the asymmetric interface between the D fragments in the cross-linked double-D structure, which is considered a prototype of the D:D interface in the fibrin protofibril. (*30*). This consistency suggests the D:D crystal contacts in the previously reported D fragment structures represent physiologically relevant interactions. Although crystal packing contacts differ in general from natural contacts (*34*), protein crystals are stable physical phases so molecular packing in the crystal may represent physiologically relevant protein−protein interactions (*35*). Indeed, previous analysis has shown that crystals with 2-fold symmetry, as in these structures, are more likely to have interfaces that resemble those in natural oligomers (*36*).

Recently, methods have been developed that may be able to determine *a priori* whether specific crystal contacts represent physiological relevant interactions (*37*). In future work it could be of interest to analyze the previous D:D crystal contacts with these methods. Because the γN308K contacts differ from the contacts in all prior structures, we would anticipate that these do not represent monomer interfaces in fibrin.

Previously, Yang et al. (*38*) proposed a model for fibrin polymerization based on the D:D structure and the crystal contacts in fibrinogen structures. In order to provide some insight into the impact of the substitution, we have incorporated the γN308K structure into the protofibril from this model (Figure 6).

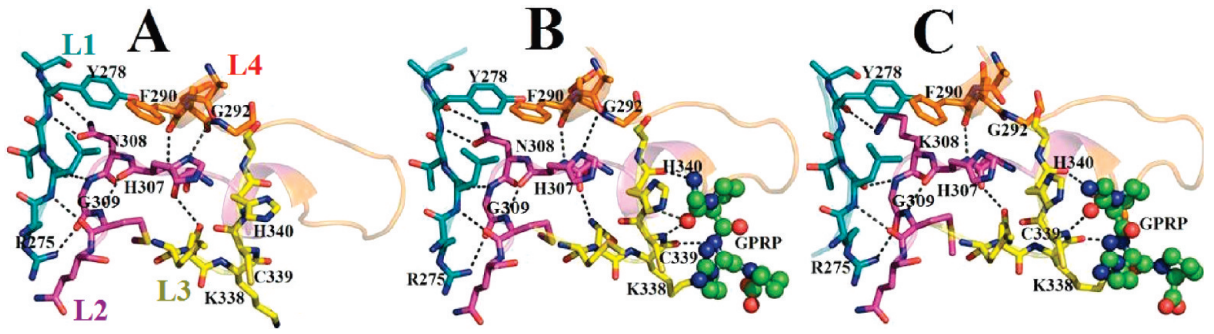

FIGURE 8: Comparison of bound and unbound forms of normal and γN308K. The conformations of γ-chain loops L1, L2, L3, and L4 are similar in the normal unbound (A), normal bound (B), and γN308K bound (C) structures, suggesting that knob "A" binding to hole "a" requires minimal motion in surrounding loops. It appears that the side-chain interactions of γ308Asn with the backbone atoms of γ278Tyr limit the flexibility of L2. Substitution with a bulkier lysine likely alters γ308Asn−γ278Tyr interaction which then affects the motion of adjacent loops and ultimately influences knob "A" binding.

With the normal, asymmetric D:D interface, the model approximates two adjacent holes "a" such that the distance between the bound portion of knobs "A" (α17−20) and the central E region is within the extended length of the missing six residues and within the constraints imposed by the α28Cys−α28Cys disulfide bond (Figure 6A). The link (α21−27) between knobs "A" (α17−20) and the central E region is indicated by the dashed lines. We incorporated the D:D crystal contact observed in γN308K into the end-to-end association of adjacent fibrin monomers, maintaining the estimated distance of ~80 Å between two strands of the protofibril as shown in Figure 6B. The different D:D contacts would put the two holes "a" on opposite sides of the junction, approximately 50 Å away from the central E region. The α17−27 link cannot span this distance, given the constraints of the α28Cys disulfide bond (Figure 6B). Thus, the new D:D crystal contacts found in γN308K are not compatible with "A:a" interactions. Assuming as we do with normal polymerization that "A:a" interactions lead to formation of the D:D interface in fibrin, we conclude that the fragment D contacts seen in the crystal packing of γN308K do not occur in the variant fibers. Rather, the D:D interface in γN308K protofibrils is asymmetric, similar to that in the cross-linked double-D structure.

Because γN308K has an increased positive surface charge, the end-to-end alignment of monomers will be destabilized by overall charge repulsion. Moreover, specific charge repulsion is apparent when two γN308K fragment D molecules are modeled onto the cross-linked double-D structure (*2*). In this structure γ308Asn is within hydrogen-bonding distance with γ321Lys in the adjacent molecule (Figure 7A). When γN308K fragment D is superimposed on each of the two D fragments in the double-D structure (Figure 7B), γ308Lys in one molecule is only ~2 Å from γ321Lys in the adjacent molecule. Hence, steric clashing and charge repulsion between these two basic residues are apparent if the variant assumes the normal D:D interface. On the basis of our structure data, we conclude that γN308K monomers cannot form stable protofibrils.

The plasmin protection assay showed weaker GPRP binding in γN308K indicating "A:a" interactions were slightly altered in the variant. Because γ308Asn does not directly interact with knob "A", it is remarkable that the γN308K substitution also impaired hole "a". We were unable to crystallize fragment D from γN308K in the absence of GPRP, so this structure is not available. However, comparison of the bound and unbound structures of normal fragment D (Figure 8A,B) showed very similar conformations in the γ-chain loops (L1 and L2) that are juxtaposed to loop 3 (L3). Loop 3 contains the γ338Lys-γ339Cys-γ340His backbone ridge that supports knob "A" binding. We note that the γ308Asn side chain interacts with the backbone atoms of γ278Tyr, which may limit the flexibility of L2 and stabilize hole "a". Substitution with lysine would alter this interaction (Figure 8C), increasing the flexibility of L2, and thus destabilize "A:a" interactions.

In summary, structural and biochemical analysis of γN308K fibrinogen leads us to conclude that altered "A:a" interactions and charge repulsion in the D:D interface destabilize protofibril formation in γN308K resulting to abnormal clot structure.

ACKNOWLEDGMENT

We thank Dr. Oleg Gorkun (University of North Carolina at Chapel Hill, Chapel Hill, NC) for helpful discussions and suggestions, Dr. Robert Immormino (Duke University, Durham, NC) for skillful assistance with the structural determination, Dr. Annie Heroux for diffraction data collection, and the National Synchrotron Light Source at Brookhaven National Laboratory for synchrotron time.

REFERENCES

1. Weisel, J. W. (2005) Fibrinogen and fibrin. *Adv. Protein Chem. 70*, 247–299.
2. Spraggon, G., Everse, S. J., and Doolittle, R. F. (1997) Crystal structures of fragment D from human fibrinogen and its crosslinked counterpart from fibrin. *Nature 389*, 455–462.
3. Cote, H. C., Lord, S. T., and Pratt, K. P. (1998) Gamma-chain dysfibrinogenemias: molecular structure-function relationships of naturally occurring mutations in the gamma chain of human fibrinogen. *Blood 92*, 2195–2212.
4. Yoshida, N., Okuma, M., Moroi, M., and Matsuda, M. (1986) A lower molecular weight gamma-chain variant in a congenital abnormal fibrinogen (Kyoto). *Blood 68*, 703–707.
5. Grailhe, P., Boyer-Neumann, C., Haverkate, F., Grimbergen, J., Larrieu, M. J., and Angles-Cano, E. (1993) The mutation in fibrinogen Bicetre II (gamma Asn308→Lys) does not affect the binding of t-PA and plasminogen to fibrin. *Blood Coagulation Fibrinolysis 4*, 679–687.
6. Okumura, N., Furihata, K., Terasawa, F., Ishikawa, S., Ueno, I., and Katsuyama, T. (1996) Fibrinogen Matsumoto II: gamma 308 Asn→Lys (AAT→AAG) mutation associated with bleeding tendency. *Br. J. Haematol. 94*, 526–528.
7. Bantia, S., Bell, W. R., and Dang, C. V. (1990) Polymerization defect of fibrinogen Baltimore III due to a gamma Asn308−Ile mutation. *Blood 75*, 1659–1663.
8. Okumura, N., Gorkun, O. V., Terasawa, F., and Lord, S. T. (2004) Substitution of the gamma-chain Asn308 disturbs the D:D interface affecting fibrin polymerization, fibrinopeptide B release, and FXIIIa-catalyzed cross-linking. *Blood 103*, 4157–4163.

9. Yoshida, N., Terukina, S., Okuma, M., Moroi, M., Aoki, N., and Matsuda, M. (1988) Characterization of an apparently lower molecular weight gamma-chain variant in fibrinogen Kyoto I. The replacement of gamma-asparagine 308 by lysine which causes accelerated cleavage of fragment D1 by plasmin and the generation of a new plasmin cleavage site. *J. Biol. Chem. 263*, 13848–13856.
10. Lord, S. T., Binnie, C. G., Hettasch, J. M., and Strickland, E. (1993) Purification and characterization of recombinant human fibrinogen. *Blood Coagulation Fibrinolysis 4*, 55–59.
11. Laemmli, U. K. (1970) Cleavage of structural proteins during the assembly of the head of bacteriophage T4. *Nature 227*, 680–685.
12. Everse, S. J., Pelletier, H., and Doolittle, R. F. (1995) Crystallization of fragment D from human fibrinogen. *Protein Sci. 4*, 1013–1016.
13. Kostelansky, M. S., Betts, L., Gorkun, O. V., and Lord, S. T. (2002) 2.8 Å crystal structures of recombinant fibrinogen fragment D with and without two peptide ligands: GHRP binding to the "b" site disrupts its nearby calcium-binding site. *Biochemistry 41*, 12124–12132.
14. Otwinowski, Z., and Minor, W. (1997) Processing of X-ray diffraction data collected in oscillation mode. *Methods Enzymol. 276*, 307–326.
15. Collaborative Computational Project, N. (1994) The CCP4 suite: programs for protein crystallography. *Acta Crystallogr. D50*, 760–763.
16. McCoy, A. J., Grosse-Kunstleve, R. W., Adams, P. D., Winn, M. D., Storoni, L. C., and Read, R. J. (2007) Phaser crystallographic software. *J. Appl. Crystallogr. 40*, 658–674.
17. Murshudov, G. N., Vagin, A. A., and Dodson, E. J. (1997) Refinement of macromolecular structures by the maximum-likelihood method. *Acta Crystallogr. D 53*, 240–255.
18. Emsley, P., and Cowtan, K. (2004) Coot: model-building tools for molecular graphics. *Acta Crystallogr. D 60*, 2126–2132.
19. Read, R. J. (1986) Improved Fourier coefficients for maps using phases from partial structures with errors. *Acta Crystallogr. A 42*, 140–149.
20. Winn, M. D., Murshudov, G. N., and Papiz, M. Z. (2003) Macromolecular TLS refinement in REFMAC at moderate resolutions. *Methods Enzymol. 374*, 300–321.
21. Krissinel, E., and Henrick, K. (2007) Inference of macromolecular assemblies from crystalline state. *J. Mol. Biol. 372*, 774–797.
22. Mullin, J. L., Gorkun, O. V., and Lord, S. T. (2000) Decreased lateral aggregation of a variant recombinant fibrinogen provides insight into the polymerization mechanism. *Biochemistry 39*, 9843–9849.
23. Lounes, K. C., Ping, L., Gorkun, O. V., and Lord, S. T. (2002) Analysis of engineered fibrinogen variants suggests that an additional site mediates platelet aggregation and that "B-b" interactions have a role in protofibril formation. *Biochemistry 41*, 5291–5299.
24. Bowley, S. R., and Lord, S. T. (2009) Fibrinogen variant BbetaD432A has normal polymerization but does not bind knob "B". *Blood 113*, 4425–4430.
25. Bowley, S. R., Merenbloom, B. K., Okumura, N., Betts, L., Heroux, A., Gorkun, O. V., and Lord, S. T. (2008) Polymerization-defective fibrinogen variant gammaD364A binds knob "A" peptide mimic. *Biochemistry 47*, 8607–8613.
26. Kostelansky, M. S., Bolliger-Stucki, B., Betts, L., Gorkun, O. V., and Lord, S. T. (2004) B beta Glu397 and B beta Asp398 but not B beta Asp432 are required for "B:b" interactions. *Biochemistry 43*, 2465–2474.
27. Kostelansky, M. S., Lounes, K. C., Ping, L. F., Dickerson, S. K., Gorkun, O. V., and Lord, S. T. (2004) Calcium-binding site beta 2, adjacent to the "b" polymerization site, modulates lateral aggregation of protofibrils during fibrin polymerization. *Biochemistry 43*, 2475–2483.
28. Kostelansky, M. S., Lounes, K. C., Ping, L. F., Dickerson, S. K., Gorkun, O. V., and Lord, S. T. (2007) Probing the gamma2 calcium-binding site: studies with gammaD298,301A fibrinogen reveal changes in the gamma294−301 loop that alter the integrity of the "a" polymerization site. *Biochemistry 46*, 5114–5123.
29. Betts, L., Merenbloom, B. K., and Lord, S. T. (2006) The structure of fibrinogen fragment D with the "A" knob peptide GPRVVE. *J. Thromb. Haemostasis 4*, 1139–1141.
30. Everse, S. J., Spraggon, G., Veerapandian, L., and Doolittle, R. F. (1999) Conformational changes in fragments D and double-D from human fibrin(ogen) upon binding the peptide ligand Gly-His-Arg-Pro-amide. *Biochemistry 38*, 2941–2946.
31. Haverkate, F., and Timan, G. (1977) Protective effect of calcium in the plasmin degradation of fibrinogen and fibrin fragments D. *Thromb. Res. 10*, 803–812.
32. Yamazumi, K., and Doolittle, R. F. (1992) The synthetic peptide Gly-Pro-Arg-Pro-amide limits the plasmic digestion of fibrinogen in the same fashion as calcium ion. *Protein Sci. 1*, 1719–1720.
33. Okumura, N., Terasawa, F., Haneishi, A., Fujihara, N., Hirota-Kawadobora, M., Yamauchi, K., Ota, H., and Lord, S. T. (2007) B:b interactions are essential for polymerization of variant fibrinogens with impaired holes "a". *J. Thromb. Haemostasis 5*, 2352–2359.
34. Carugo, O., and Argos, P. (1997) Protein-protein crystal-packing contacts. *Protein Sci. 6*, 2261–2263.
35. Lo Conte, L., Chothia, C., and Janin, J. (1999) The atomic structure of protein-protein recognition sites. *J. Mol. Biol. 285*, 2177–2198.
36. Janin, J., and Rodier, F. (1995) Protein-protein interaction at crystal contacts. *Proteins 23*, 580–587.
37. Bernauer, J., Bahadur, R. P., Rodier, F., Janin, J., and Poupon, A. (2008) DiMoVo: a Voronoi tessellation-based method for discriminating crystallographic and biological protein-protein interactions. *Bioinformatics* (*Oxford, England*) *24*, 652–658.
38. Yang, Z., Mochalkin, I., and Doolittle, R. F. (2000) A model of fibrin formation based on crystal structures of fibrinogen and fibrin fragments complexed with synthetic peptides. *Proc. Natl. Acad. Sci. U.S.A. 97*, 14156–14161.